SEMI-THERM®
THERMAL INNOVATIONS THAT MAKE THE WORLD'S TECHNOLOGY COOL...

Thermal performance of PHP heat spreader at central and non-central heat load configuration

Sai Kiran Hota*, Nathan Van Velson, Srujan Rokkam
Advanced Cooling Technologies, 1046 New Holland Ave Building 2
Lancaster, PA. USA. 17601
Saikiran.hota@1-act.com

Abstract

Pulsating heat pipe (PHP)-embedded heat spreaders are increasingly employed to manage high heat fluxes from electronics chips. Previous studies have characterized their performance under symmetrical heat-transfer paths with a centrally located heat source and edge heat rejection (center-to-edge configuration). This investigation examines the heat-transfer behavior of a PHP heat spreader under a non-central heat-source placement, while maintaining standard edge cooling. The heat source was offset 5 mm to the right of the spreader center. Testing was conducted with standard cooling on both edges (ON mode), cooling only the right edge (−11 ON mode), and cooling only the left edge (−7 ON mode) at flange temperatures of -10°C and 0°C. Key findings are as follows: under ON mode, the PHP operated normally, with preferential heat transfer to the right side due to the active evaporator–condenser pair. In −11 ON mode, only the right-side exhibited PHP operation, while the left side remained adiabatic and functioned as a working-fluid reservoir. Under −7 ON mode, the PHP did not operate. In vertical orientations, the PHP demonstrated similar behavior as in horizontal mode under ON conditions but did not operate under either −11 ON or −7 ON modes at 0°C flange set point.

Keywords—electronics cooling, passive cooling, two-phase heat transfer, pulsating heat pipe, heat pipe

I. Introduction

Electronics computing power has increased substantially in recent years while device size has continued to shrink. As a result, electronic chips now dissipate heat fluxes well above tens of W/cm^2. The electronics cards must be maintained below 75°C to ensure safe and reliable operation [1]. Conventional cards that rely on metal conduction plates such as aluminum plates cannot sustain such high heat fluxes without experiencing elevated temperatures. To address this thermal challenge, Cu-H_2O heat-pipe-embedded thermal spreaders have been investigated. Depending on the form factor, these devices can provide 2-5x improvement in thermal performance compared to pure conduction solutions [2, 3]. While effective, they are suitable primarily when the heat-rejection temperature (condenser) is above 5°C and when heat spreading is largely planar, with only limited capability for three-dimensional (3D) spreading under modest curvature [4]. Vapor chamber is another high thermal performance solution capable of handling large heat fluxes [5]. Typically made from copper, they also operate effectively only above approximately 5°C and are often heavier and more expensive than conventional approaches [6]. Moreover, vapor chambers function predominantly as two-dimensional spreaders, and realizing complex 3D geometries remains challenging. Given the emerging need for high-heat-flux thermal management in cold environments (below 0°C) and under strict form-factor constraints such as 90° turns, pulsating heat-pipe (PHP)-embedded heat spreaders are now being explored. These devices incorporate capillary-scale serpentine channels within the base plate. In addition to high thermal performance and low-temperature capability, PHP spreaders offer significant mass savings [7]. For small- to medium-scale form factors, PHP heat spreaders have demonstrated more than 2-5x improvement in thermal conductance compared with conduction plates, similar to embedded heat-pipe solutions [7, 8, 9].

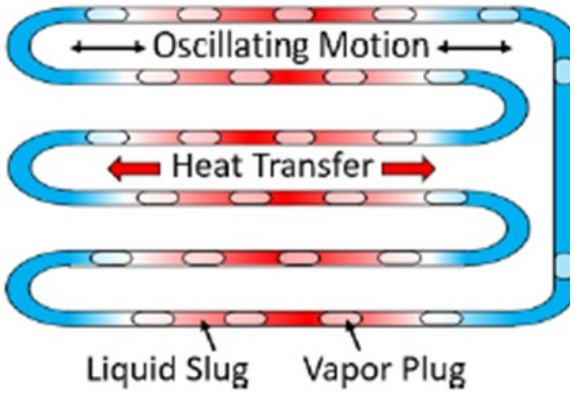

Figure 1. Conceptual schematic illustrating operation of a pulsating heat pipe

PHP is a passive two-phase heat-transfer device consisting of capillary-sized, meandering serpentine channels that connect the heat source and heat-rejection regions. Figure 1 shows a conceptual schematic of PHP operation. The channel is evacuated and then charged with a saturated working fluid. The fluid distributes itself into liquid slugs and vapor plugs. During operation, the pressure differential between the hot and cold ends balanced by various thermo-hydraulic forces acting on each liquid slug drives passive oscillatory (or sometimes circulatory) motion of the working fluid [10, 11]. The operational heat-transfer limits are governed by the PHP geometry, particularly the

Resrach supported by NASA SBIR Phase II contract #80NSSC2CA205.
Corresponding author contact can be reached here by e-mail: saikiran.hota@1-act.com; or Ph: (717-305-4062).

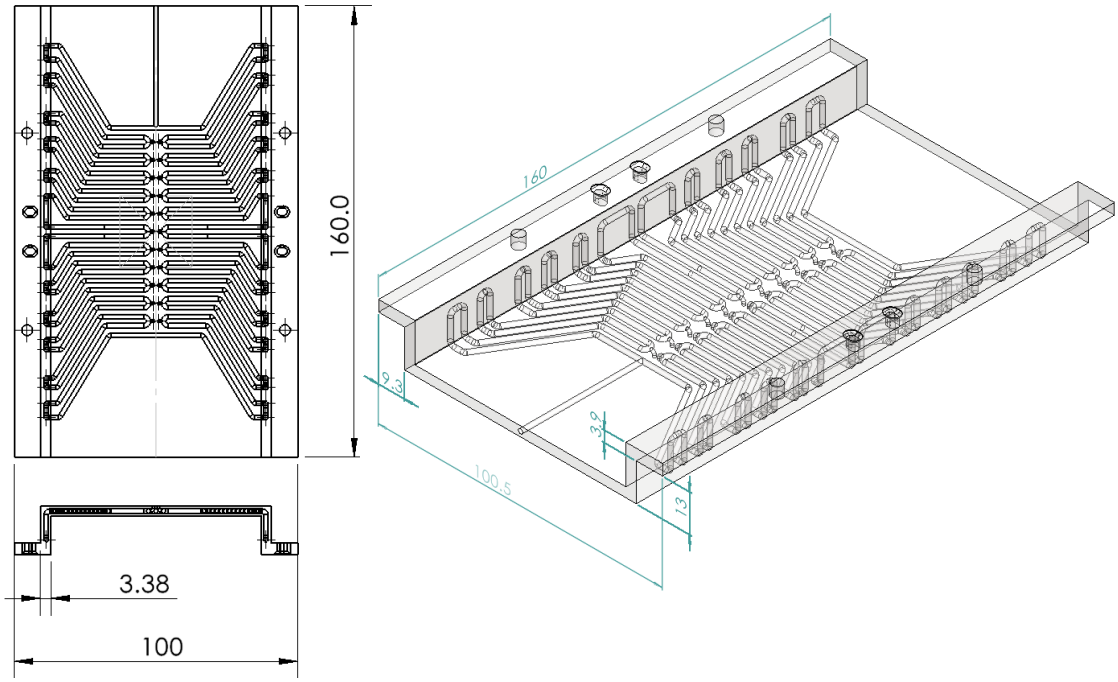

Figure 2. Geometric description of PHP heat spreader

channel diameter, and by the working-fluid properties [12, 13]. Based on these limits and on performance-based merit number analyses [14, 15], ammonia and propylene are the most suitable working fluids for electronics applications.

Previous investigations demonstrated that a propylene PHP embedded heat spreader provided 2x improvement in heat transfer capability for 3U-form factor electronics below 0°C [16]. Additionally, the device exhibited gravity-independent operation under central heat-source conditions. Thermal-performance testing with ammonia as the working fluid showed greater than a two-fold increase in thermal conductance and a heat-transport capacity exceeding 300 W [17]. The ammonia PHP spreader also demonstrated gravity-independent performance in vacuum environments, indicating its feasibility for space systems [18].

This manuscript extends the investigation of an ammonia PHP heat spreader designed for 3U-form-factor electronics, using the geometry presented in [18]. Rather than focusing on performance improvements relative to conventional solutions (discussed in [17, 18]), this work examines the operational characteristics of the PHP under an offset-center heat-load configuration (partially discussed in [19]), in which the heat source is deliberately placed away from the geometric center. The resulting heat-transfer behavior provides critical insights for thermal control and system integration.

II. Description of Electronics Card and Methods

A 3U-form-factor electronics card with dimensions of 160 mm × 100 mm × 3.38 mm was selected for thermal performance testing. The PHP heat spreader was additively manufactured as a single unit using aluminum alloy ($AlSi_{10}Mg$). The geometric details of the heat spreader are shown in Figure 2. A vertical step located approximately 9.3 mm from the card edges, forms flanges that interface with the cold plate through a card retainer. The PHP channel diameter was 1.52 mm, selected based on design analysis confirming Bond-number requirements for liquid-slug formation and ensuring a four-fold safety factor for the high-pressure working fluid. The flanges were fully solid, and the fluid-channel layout was originally designed for standard central heat-load testing. In this manuscript, the PHP heat spreader was tested using an offset center heat-load configuration as shown in Figure 3. The standard center heat load configuration is also shown for reference. In the offset setup, the heat source, a 25.4 mm x 25.4 mm aluminum block with cartridge heater rod inserts was shifted to the right, placing its closest edge 5 mm from the center of the heat-source plane (electronics). This reduced the heat-transfer distance from the heat-source center to the right side and increased it on the left side. A key consequence of this offset is that the heat load is applied (biased) only to the right-side PHP pair. The left-side participates in heat transfer when cooling is applied normally on both flanges. As shown later, if cooling is applied only on the right side, the left side of the heat spreader is adiabatic and only acts as a potential reservoir for the working fluid.

PHP operational characteristics were inferred from the wall-temperature profile measured using type-T thermocouples. Thermocouples 1-3 recorded the heat source interface by being held in place by spring-plunger mounts. Thermocouples 7 and 11 measured the left and right flange temperatures. Thermocouples 19 and 20 were added specifically for this study to estimate the PHP condenser temperature under offset-load conditions (these

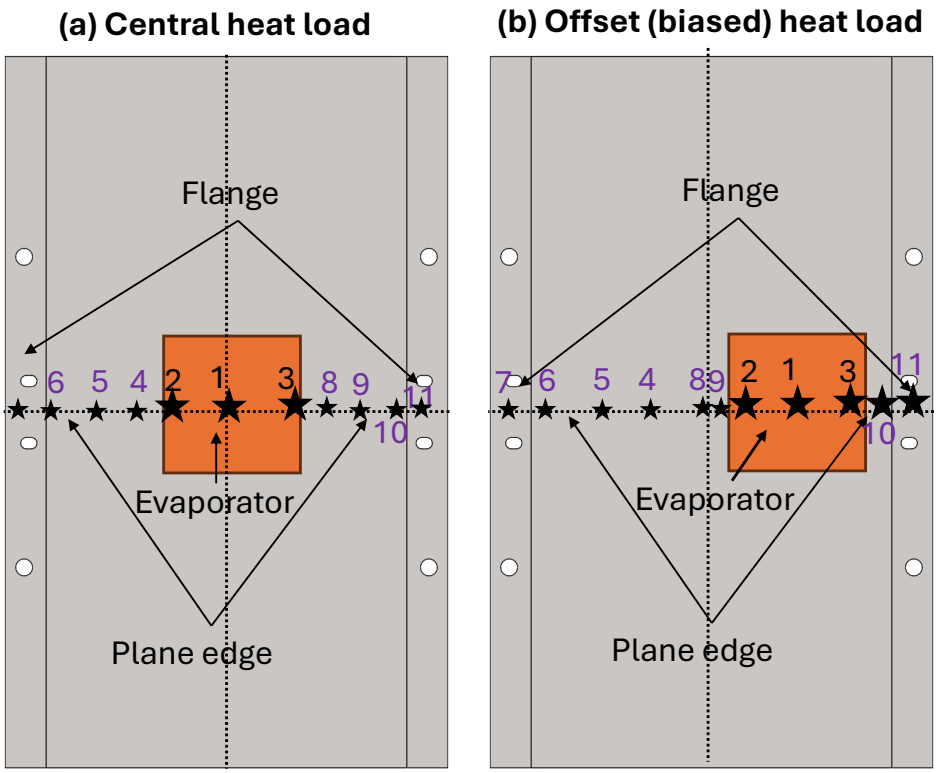

Figure 3. Graphical illustration of center (conventional) and offset (biased) center heat load configuration

were not used during the standard central load testing). The other thermocouples 4-6 and 8-10 are adiabatic in the central heat configuration. Thermocouples 4–6 and 8–10 were adiabatic in the standard setup. Under offset heat loading, Thermocouple 9 was positioned near the U-bend of the right-side PHP pair, where the wall-temperature behavior approached that of the heat source because of the local working-fluid motion. Thermocouple 8 was likely located at the geometric center of the spreader, in the solid region between the left and right PHP pairs.

Thermal performance testing followed a quasi-steady-state procedure with incremental increases in heat load. Testing continued until the heat-source temperature reached 85 ± 5°C. Higher cutoff temperatures were necessary due to delayed PHP start-up under offset loading, which occasionally resulted in peak temperatures exceeding 80°C. The flange temperature setpoint was held at either −10°C or 0°C, and tests were performed with the heat spreader in both horizontal and vertical orientations. Ammonia, charged to a fill ratio of 64% (referenced to room temperature), was used as the working fluid.

The test conditions were:

- **Horizontal** orientation: both flanges cooled (ON mode), only right flange cooled (-11 ON), or only left flange cooled (-7 ON).
- Vertical orientation, tilted to the right (-11 g): represents top heated mode as the evaporator is located directly above the corresponding condenser. Tested in ON mode, -11 ON mode, and – 7 ON mode.
- Vertical orientation, tilted to the left (-7 g): represents bottom heat mode as the evaporator is below the corresponding condenser. Tested in ON mode, -11 ON mode, and – 7 ON mode.

In the -11 ON mode, only the right-side evaporator-condenser pair was active. In -7 ON mode, the thermal path

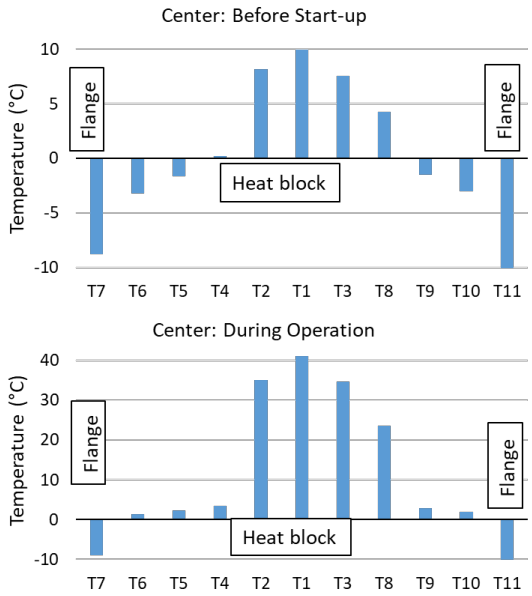

Figure 4. Temperature profile of PHP heat spreader under nominal center heating configuration

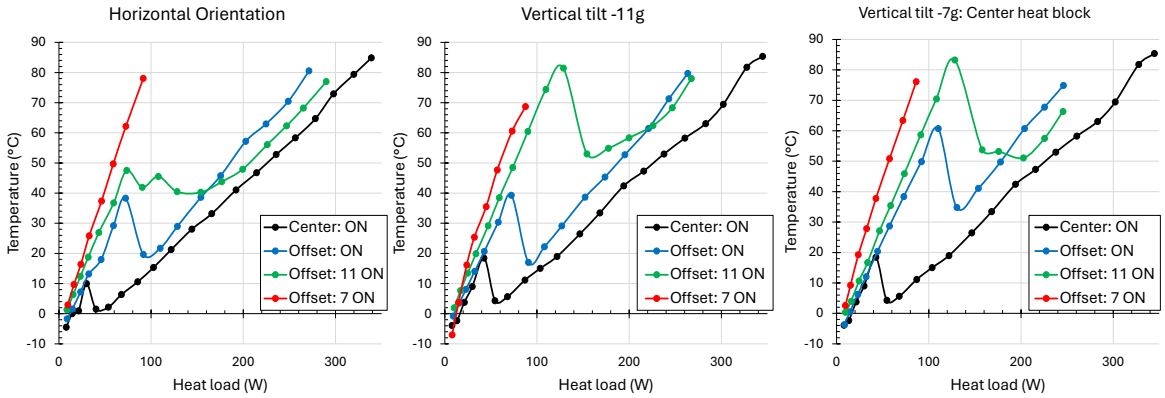

Figure 5. Instantaneous steady-state evaporator Temperature profile (thermocouple-1) variation with heat load

consisted of an evaporator–adiabatic sequence on one side and an adiabatic–condenser sequence on the other.

III. HEAT TRANSFER CHARACTERISTICS WITH CENTRAL HEATING: REFERENCE CASE

A reference set of PHP heat transfer characteristics was established for the nominal central heating case. Figure 4 shows the temperature profile of the heat spreader prior to PHP start-up at a 30 W heat load and during stable two-phase operation at 200 W, with the flanges maintained at -10°C in horizontal orientation. During two-phase operation, the PHP heat spreader exhibited a symmetric wall-temperature profile. The only deviation occurred at Thermocouple 8, which recorded a higher temperature due to unintended thermal-tape contact with the heater block, representing an experimental inconsistency. The PHP heat spreader successfully transported up to 340 W while maintaining a peak temperature below 85°C. The wall temperature profile was symmetrical across both left and right side of the device.

Additionally, reference temperature profiles were obtained at a flange temperature of 0°C at both horizontal and vertical orientation. Similar symmetric heat-transfer behavior was observed for these reference central-load configurations.

IV. HEAT TRANSFER CHARACTERISTICS OF THE PHP HEAT SPREADER UNDER OFFSET CENTER HEAT LOADING

Following the reference testing under central heating, the heat source was shifted to the right, with a separation of 5 mm from the heat-spreader center to the nearest edge of the heater block. Figure 5 the instantaneous quasi-steady-state evaporator temperature at Thermocouple 1 (center of heat source) for a flange temperature of -10°C. The corresponding evaporator temperature profile at a flange temperature of 0°C is shown in Figure 6. Compared with the reference central-load case, the start-up power required and the resulting evaporator temperature under incremental heat loading were lower in the reference case. This is because the heat flux on the evaporator–condenser pair was lower and more evenly distributed between the left and right sides of the evaporator. With the heater block offset to the right, conventional ON-mode testing showed effective PHP operation, but with higher start-up power requirements and elevated evaporator temperatures. The maximum heat-carrying capacity under offset conditions was 260±10 W at -10°C and below 250 W at 0°C. Notably, the start-up power requirement was more than twice that of the reference case for most experimental conditions. Under -11 ON mode, the PHP heat spreader operated less effectively resulting in significant deviation in evaporator temperature before start-up. After start-up, however, at flange setpoints of -10°C in all orientations and 0°C in horizontal orientation, the

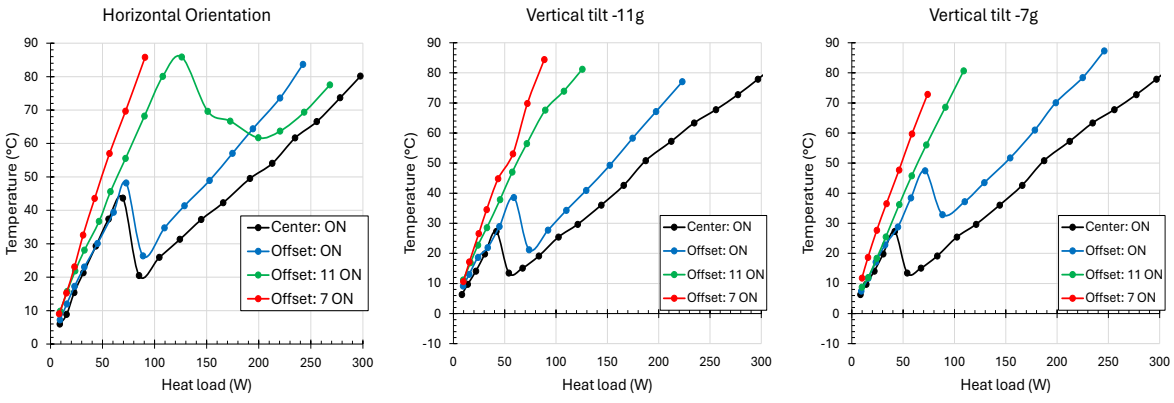

Figure 6. Instantaneous steady-state evaporator Temperature profile (thermocouple-1) variation with heat load

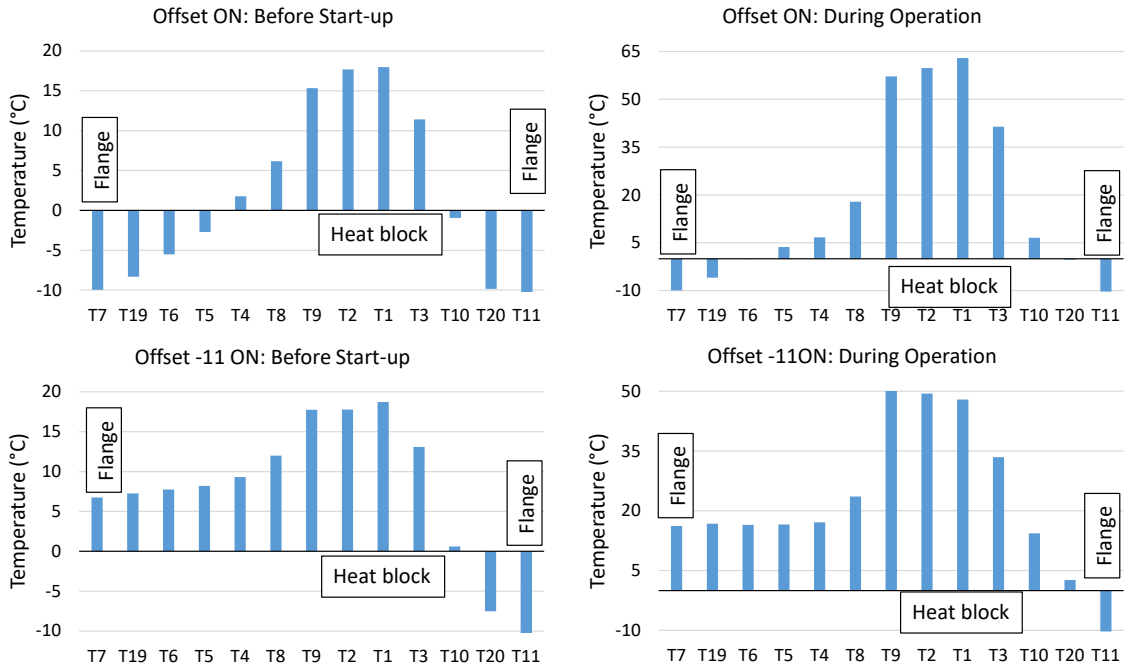

Figure 7. Temperature profile of PHP heat spreader under offset center heat load condition in horizontal orientation at -10°C flange temperature

evaporator temperatures converged, indicating similar overall heat-dissipation behavior. Closer inspection of the temperature profiles (Figure 7 to Figure 9) revealed that majority of heat transfer occurred on the right side of the heat spreader. In −7 ON mode, the PHP heat spreader did not operate.

Figure 7 shows the instantaneous quasi-steady-state temperature profile under the offset-center heat-load condition with a flange temperature of -10°C. The heat loads for the "before start-up" and "during operation" scenarios were 30 W and 200 W, respectively, in horizontal orientation testing. Vertical orientations are labeled −11 g or −7 g according to tilt direction. Before start-up, heat transfer was primarily via solid-wall conduction, resulting in a relatively uniform temperature gradient. In ON mode, normal PHP two-phase operation was observed, with a significant fraction of heat transferred through the right-side evaporator–condenser pair. The proximity of the right-side flange influenced Thermocouple 3 readings. The left side also participated in heat transfer, as indicated by the gradient between Thermocouple 8 at the center and Thermocouple 7 at the left flange. Similar behavior persisted at peak heat loads up to 270 W. In -11 ON mode, coolant flow to the left flange was disabled, resulting in higher temperatures on the left compared with the right flange. Prior to PHP start-up, the temperature profile showed a slight gradient, indicating minimal heat transfer on the left side. After start-up, the high thermal conductivity from the active right-side evaporator–condenser pair led to nearly all heat being transferred through the right side, while the left side was adiabatic with less than 1°C temperature gradient from center to the flange.

Similar observations were made under vertical tilt at flange temperature of -10°C, as shown in Figure 8. The temperature profile was found to be largely independent of gravity. In ON mode, the temperature profiles were largely similar with up to 5-10°C differences at the evaporator, , attributable to factors such as gravity, evaporator–condenser positioning, and working-fluid slug distribution. Despite this, the overall temperature gradient from the heat-spreader center to the flanges was consistent across tilt directions. In -11 ON mode heat transfer occurred solely through the right-side evaporator–condenser pair, while the left side remained effectively adiabatic.

At a flange temperature of 0°C, similar temperature profiles were obtained in both horizontal and vertical orientations, as shown in Figure 9. In the horizontal orientation, the gradient pattern resembled that observed at −10°C. In vertical orientations, however, the PHP heat spreader did not operate under biased cooling conditions (−11 ON or −7 ON modes).

V. Conclusions

Thermal testing of a 3U-form-factor PHP heat spreader was performed under an offset-center heat-load configuration, representing a non-central electronics heat source placement for a spreader originally designed for central loading. The nearest edge of the heat source was positioned 5 mm from the center of the heat spreader, closer to the right-side flange. Testing was conducted in both horizontal and vertical orientations at flange temperatures of -10°C and 0°C using ammonia as the working fluid at a 64% fill ratio.

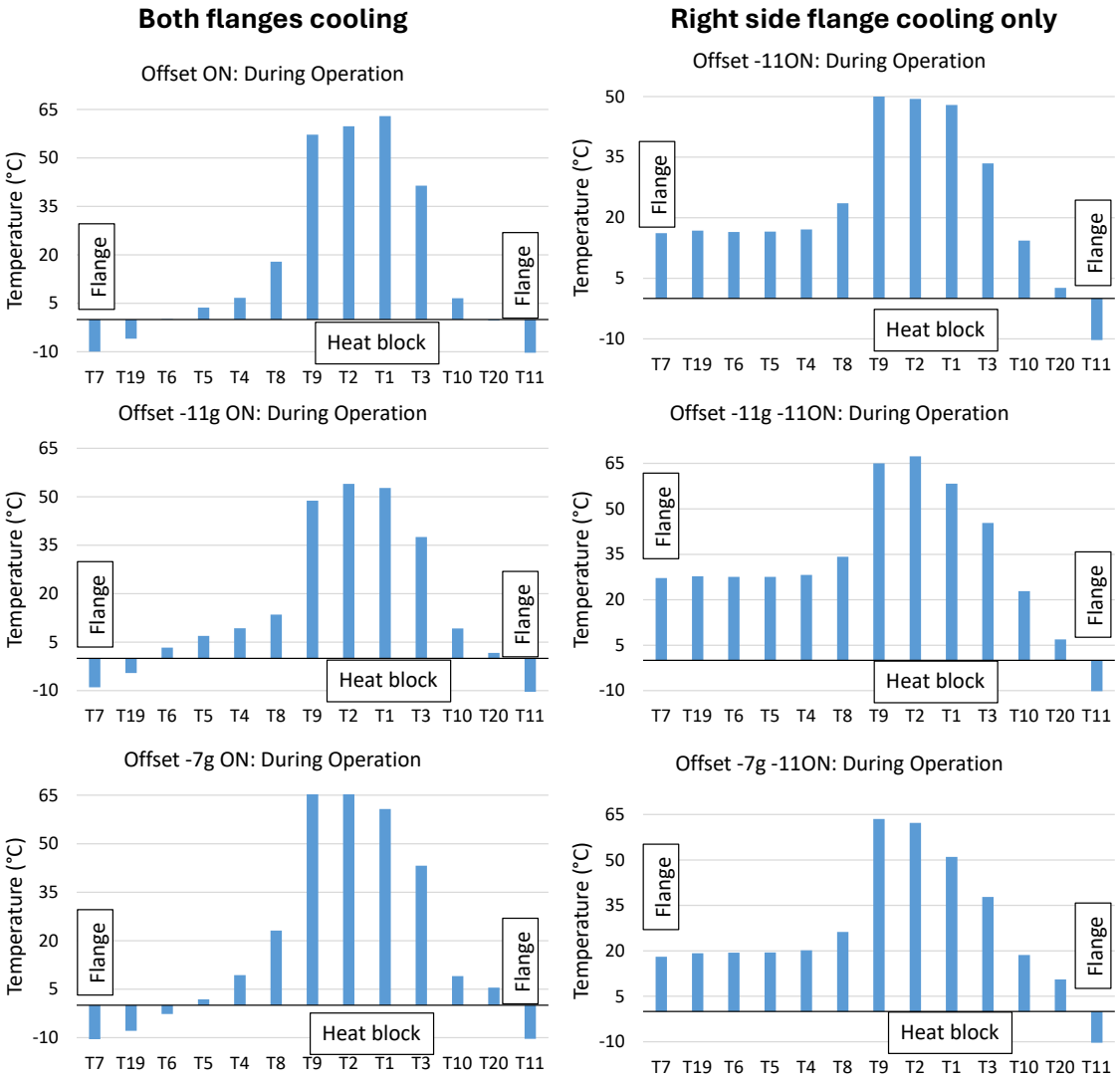

Figure 8. Temperature profile of PHP heat spreader at 200 W heat load in horizontal orientation and vertical (-11g & -7g) orientation

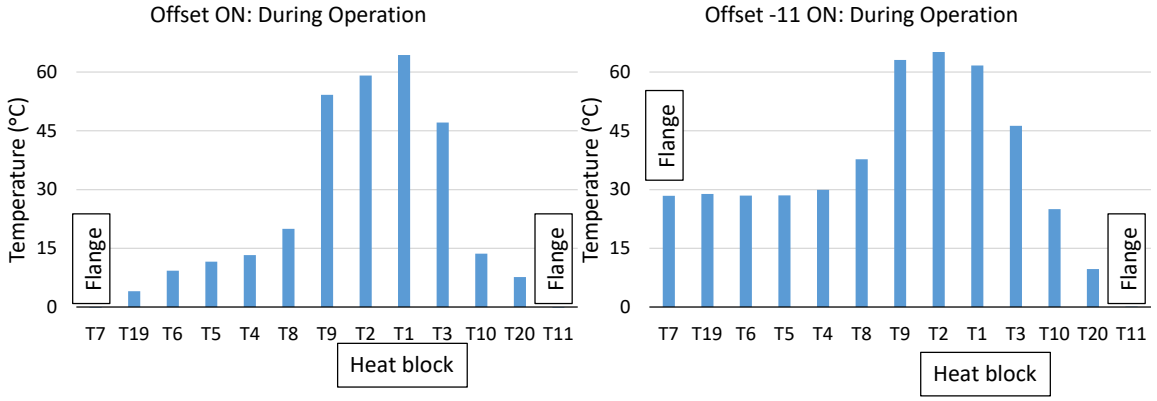

Figure 9. Temperature profile of PHP heat spreader under offset center heat load condition in horizontal orientation at 0°C flange temperature

Table 1. Maximum operating conditions achieved under offset center heat load configuration

Flange temperature	-10°C			0°C		
	ON	11ON	7ON	ON	11ON	7ON
Horizontal	80.5°C @ 270W	78.5°C @ 265W		83°C @ 240W	84°C @ 220W	
Vertical: -11g tilt	85°C @ 265W	87.5°C @ 268W		83.5°C @ 225W		
Vertical: -7g tilt	87°C @ 265W	82°C @ 245W		87.5°C @ 240W		

Table 1 summarizes the operating conditions under which the PHP heat spreader functioned in different thermal-control modes (ON, −11 ON, and −7 ON) for both orientations. Overall, the heat-transfer characteristics were similar in horizontal and vertical orientations. In ON mode, most of the heat was transferred through the right-side evaporator–condenser channels, while the left side contributed minimally due to continuous cooling. In −11 ON mode, coolant flow to the left flange was disabled, rendering the left side effectively adiabatic. Prior to PHP start-up, the left-side temperature profile exhibited a slight gradient, indicating minor heat transfer. After start-up, the high thermal conductivity of the active right-side evaporator–condenser pair ensured that nearly all heat was carried through the right side, with temperature differences between the two sides reduced to less than 1 °C. In −7 ON mode, the PHP heat spreader did not operate.

ACKNOWLEDGMENT

The work presented here was performed under the NASA SBIR Phase II program, contract #80NSSC22CA205. The authors thank Dr. Sergey Y. Semenov, NASA Program Manager, for his valuable feedback in enabling this work. The authors also express their gratitude to Mr. Eugene Sweigart and Mr. Justin Boyer for their support in conducting the experiments. Appreciation is further extended to Dr. Kuan-Lin Lee and Dr. Ramy Abdelmaksoud for their contributions throughout the program.

REFERENCES

[1] "Reliability prediction of electronic equipment.," U.S. Department of Defense, MIL-HDBK-2178B, NTIS, 1974., Springfield, VA;, 1974.

[2] S. K. Hota, K.-L. Lee, G. Hoeschele, R. Bonner and S. Rokkam, "Experimental comparison on thermal performance of pulsating heat pipe and embedded heat pipe heat spreaders," in *39th Semiconductor Thermal Measurement, Modeling & Man*, 2023.

[3] S. K. Hota, K.-L. Lee, G. Hoeschele, R. W. Bonner and S. Rokkam, "Performance investigation on different form factor embedded heat pipe and pulsating heat pipe heat spreaders," in *Proceedings of 17th International Heat Transfer Conference*, 2023.

[4] N. Van Velson, S. K. Hota, G. Hoeschele and S. Rokkam, "Practical Considerations for Pulsating Heat Pipe and Embedded Heat Pipe Heat Spreaders," in *PCIM Conference 2025; International Exhibition and Conference for Power Electronics, Intelligent Motion, Renewable Energy and Energy Management*, Nürnberg, Germany, 2025.

[5] Y. Varol, H. Coşanay, E. Tamdoğan, M. Parlak, Ş. M. Şenocak and H. F. Oztop, "Vapor chamber thermal performance: Partially heated with different heating areas at the center and supported by numerical analysis for the experimental setup," *Applied Thermal Engineering,* vol. 260, p. 124978, 2025.

[6] [Online]. Available: https://www.1-act.com/resources/blog/when-to-use-heat-pipes-hik-plates-vapor-chambers-and-conduction-cooling/?srsltid=AfmBOopS3EozhxLhKKQSxtYaBGvEwCg1wZssd4c3WVFT8ltbybtnP06n.

[7] K.-L. Lee, S. K. Hota, A. Lutz and S. Rokkam, "Advanced Two-Phase Cooling System for Modular Power Electronics," in *51st International Conference on Environmental Systems*, St. Paul, MN, USA, 2022.

[8] S. K. Hota, K.-L. Lee, B. Leitherer, G. Elias, G. Hoeschele and S. Rokkam, "Pulsating heat pipe and embedded heat pipe heat spreaders for modular electronics cooling," *Case Studies in Thermal Engineering,* vol. 49, p. 103256, 2023.

[9] R. Abdelmaksoud, J. Diebold, S. K. Hota, K.-L. Lee, S. Sinha and D. Maksimovic, "Development of ceramic pulsating heat pipes for medium-voltage power electronics," in *International Electronic Packaging Technical Conference and Exhibition Vol. 87516 American Society of Mechanical Engineers*, 2023.

[10] S. K. Hota, K.-L. Lee, T. McFarland, G. Hoeschele, J. Weyant and S. Rokkam, "High performance heat spreader for thermal management of high heat flux optical and electronics systems," in *Proc. SPIE 12894, Next-Generation Optical Communication: Components, Sub-Systems, and Systems XIII, 128940N*, San Francisco, 2024.

[11] S. Ouchi, K. Kurose and K. Miyata, "Mechanism of transition between oscillating and pulsating–circulating flows in bottom-heated pulsating heat pipe based on simple simulation model," *International Journal of Thermal Sciences,* vol. 217, p. 110035, 2025.

[12] S. K. Hota, K.-L. Lee, G. Hoeschele, T. Mcfarland, S. Rokkam and R. Bonner, "Experimental comparison of two-phase heat spreaders for space modular electronics," in *52nd International Conference on Environmental Systems*, 2023, 2023.

[13] B. Drolen and C. Smoot, "Performance limits of oscillating heat pipes: Theory and validation," *Journal of Thermophysics and Heat Transfer,* vol. 31, no. 4, 2017.

[14] J. Kim and S. Kim, "Experimental investigation on working fluid selection in a micro pulsating heat pipe," *Energy Conversion and Management,* vol. 205, p. 112462, 2020.

[15] S. K. Hota, K.-L. Lee, G. Hoeschele, T. Mcfarland and S. Rokkam, "Development of Modular 3U Form Factor Pulsating Heat Pipe Based Plate Heat Spreader for Electronics Cooling," in *53rd International Conference on Environmental Systems*, Louisville, KY,USA, 2024.

[16] S. K. Hota, K.-L. Lee, G. Hoeschele and S. Rokkam, "Investigation on Pulsating Heat Pipe (PHP) Heat Spreader Plate for Electronics Cooling," in *2024 40th Semiconductor Thermal Measurement, Modeling & Management Symposium (SEMI-THERM)*, 2024.

[17] S. K. Hota, K.-L. Lee, R. Abdelmaksoud and S. Rokkam, "High Performance 3U-Form Factor Pulsating Heat Pipe Heat Spreader," in *41st Semiconductor Thermal Measurement, Modeling & Management Symposium (SEMI-THERM)*, 2025.

[18] S. K. Hota, K.-L. Lee, R. Abdelmaksoud, N. Van Velson and S. Rokkam, "Thermal Performance Characterization of Pulsating Heat Pipe Based Electronics Heat Spreaders," in *54th Internatonal Conference on Environmental Systems*, 2025.

[19] S. K. Hota, R. Abdelmaksoud, K.-L. Lee, S. Rokkam and N. V. Velson, "Experimental Investigation on Three-Dimensional Pulsating Heat Pipe Emebedded Electronics Heat Spreader and Enclosure," *Thermal Science and Engineering Progress,* (In Review).